Webster, J.M., Ravelo, A.C., Grant, H.L.J., and the Expedition 389 Scientists
Proceedings of the International Ocean Discovery Program Volume 389
publications.iodp.org

Site M0100[1]

J.M. Webster, A.C. Ravelo, H.L.J. Grant, M. Rydzy, M. Stewart, N. Allison, R. Asami, B. Boston, J.C. Braga, L. Brenner, X. Chen, P. Chutcharavan, A. Dutton, T. Felis, N. Fukuyo, E. Gischler, S. Greve, A. Hagen, Y. Hamon, E. Hathorne, M. Humblet, S. Jorry, P. Khanna, E. Le Ber, H. McGregor, R. Mortlock, T. Nohl, D. Potts, A. Prohaska, N. Prouty, W. Renema, K.H. Rubin, H. Westphal, and Y. Yokoyama[2]

[1] Webster, J.M., Ravelo, A.C., Grant, H.L.J., Rydzy, M., Stewart, M., Allison, N., Asami, R., Boston, B., Braga, J.C., Brenner, L., Chen, X., Chutcharavan, P., Dutton, A., Felis, T., Fukuyo, N., Gischler, E., Greve, S., Hagen, A., Hamon, Y., Hathorne, E., Humblet, M., Jorry, S., Khanna, P., Le Ber, E., McGregor, H., Mortlock, R., Nohl, T., Potts, D., Prohaska, A., Prouty, N., Renema, W., Rubin, K.H., Westphal, H., and Yokoyama, Y., 2025. Site M0100. In Webster, J.M., Ravelo, A.C., Grant, H.L.J., and the Expedition 389 Scientists, Hawaiian Drowned Reefs. Proceedings of the International Ocean Discovery Program, 389: College Station, TX (International Ocean Discovery Program). https://doi.org/10.14379/iodp.proc.389.107.2025

[2] **Expedition 389 Scientists' affiliations.**

Contents

Keywords
International Ocean Discovery Program, IODP, Expedition 389, *MMA Valour*, Hawaiian Drowned Reefs, Earth climate system, Earth system feedbacks, Earth history tipping points, Site M0100, coral reef, volcanics, sea level, paleoclimate, central Pacific, reef health, Hawaiian geology, basalt, lava, carbonates, Kawaihae

Core descriptions

Supplementary material

References (RIS)

MS 389-107
Published 26 February 2025

Funded by ECORD, JAMSTEC, and NSF OCE1326927

1. Operations

The multipurpose vessel *MMA Valour* was used as the drilling platform throughout Expedition 389. At all Expedition 389 sites, dynamic positioning (DP) was used to provide accurate positions throughout operations and water depth was established using a Sound Velocity Profiler (SVP) placed on the top of the PROD5 drilling system. For more detail on acquisition methods, see **Introduction** in the Expedition 389 methods chapter (Webster et al., 2025a).

Summary operational information for Site M0100 is provided in Table **T1**. All times stated are in Hawaiian Standard Time (HST).

1.1. Hole M0100A

Site M0100 was the first operational site following the midexpedition port call to Barbers Point Harbor on 28 and 29 September 2023. The *MMA Valour* arrived on site at 0230 h on 30 September, and DP trials were completed by 0245 h. At 0625 h, PROD5 was launched. While looking for a landing site 10 m above the seabed, instrumentation indicated an oil pressure drop, and PROD5 was recovered for repairs on deck at 1043 h. After repairs to a faulty manifold valve, PROD5 was relaunched at 1135 h. Rotary coring and casing commenced in Hole M0100A at 1300 h at a water depth of 998.0 m. At 0508 h on 1 October, coring had advanced to 12.43 meters below seafloor (mbsf) when the bridge initiated a yellow alert due to a heading problem on the vessel, and the PROD5 Control started recovering pipes from the ground. At 0514 h, a red alert was initiated by the vessel due to a total loss of satellite connection to both Differential Global Positioning Systems (DGPS) and loss of vessel position. Hole M0100A was abandoned immediately. PROD5 was lifted off the seabed with all drill pipes, leaving 7.50 m of casing in the ground with 1 m protruding above the seabed. At 0545 h, approval from the bridge was given to recover PROD5 once the DGPS sensors were operating correctly, and PROD5 was recovered to deck at 0705 h. On-deck operations

Table T1. Hole summary, Site M0100. R = rotary coring mode. LAT = Lowest Astronomical Tide. **Download table in CSV format.**

Hole	Water depth (mbsf)	Date started (2023)	Date finished (2023)	Latitude	Longitude	Coring method	Total drilled depth (m)	Recovered length (m)	Core recovery (%)	Cores (*N*)	Notes
389-M0100A	998.0	30 Sep	01 Oct	20.137606°	–156.079107°	R	12.43	9.73	78.28	12	LAT water depth: 997.4 m. Borehole abandoned due to vessel technical issues.

commenced, and core barrels were extracted for curation. Following the loss of DGPS, both the vessel operator and PROD5 operator put operations on hold until investigations were complete. During the suspension of coring operations, the transit to Site M0101 was initiated at 1330 h with arrival at Site M0101 at 1930 h on October 1.

A total of 12 cores were recovered from Hole M0100A from 12.43 m of rotary coring, with a total recovered core length of 9.73 m (78.28% recovery).

2. Lithostratigraphy

Hole M0100A spans 0.00–12.43 mbsf and was cored in the Kawaihae region, in the vicinity of Mahukona, at 998 meters below sea level (mbsl). It includes an upper portion of coralgal boundstone underlain by a volcanic sequence of in-place lavas, welded volcanic breccias, and volcaniclastic detritus.

2.1. Hole M0100A

In Hole M0100A (Figure **F1**), coralgal boundstone (Figure **F2A**) was recovered from 0.00 to 0.13 mbsf, consisting of *Porites* (columnar or branching) encrusted with crustose coralline algae (CCA). A few grainstone clasts were also recovered. There was no recovery from 0.13 to 1.80 mbsf. From 1.80 to 1.98 mbsf, algal boundstone (Figure **F2B**) was recovered; it consists of CCA and fruticose coralline algae (FCA). A sharp contact at 1.98 mbsf separates the algal boundstone from the underlying lava. Within the lava, the uppermost interval is in-place lava flow, with a rounded upper surface that is encrusted with coralline algae and infilled in both cracks and vesicles with bioclastic sediment, indicating that the lava provided the substrate for subsequent biogenic encrustation and bioclastic deposition. The lava is fragmented, is mildly altered on many of the broken surfaces, has a porphyritic (up to 5% olivine phenocrysts and less abundant phenocrysts of clinopyroxene) texture, and has a phaneritic to aphanitic groundmass. Vesicles occur in two pop-

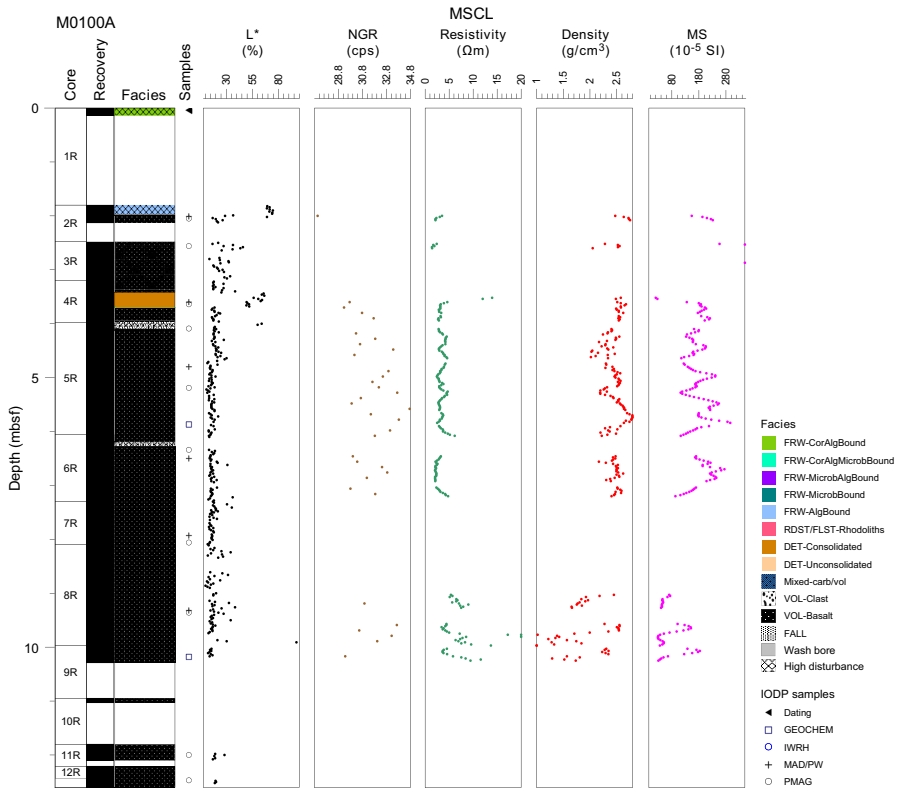

Figure F1. Lithostratigraphy and MSCL data, Hole M0100A. cps = counts per second, MS = magnetic susceptibility. NGR = natural gamma radiation.

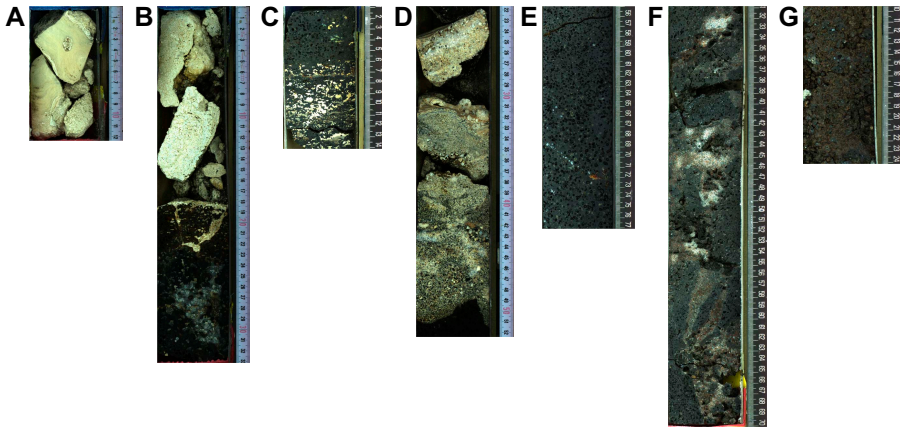

Figure F2. Lithologies, Hole M0100A. A. Fragments of coralgal boundstone (1R-1, 0–13 cm). B. Fragments of algal boundstone and lava (2R-1, 0–33 cm). C. Lava, including a prominent zone with vesicles filled in by bioclastic sediments (3R-1, 1–14 cm). D. Consolidated bioclastic grainstone (4R-1, 23–50 cm). E. Porphyritic basaltic lava with large, prominent olivine phenocrysts, minor clinopyroxene, and abundant round, millimeter-sized vesicles (6R-1, 56–77 cm). F. Brecciated lava with subrounded clasts in an oxidized matrix (5R-1, 30–70 cm). G. Lava with reddish stain (8R-1, 10–24 cm).

ulations: a dominant, round, millimeter-sized fraction and a less abundant, centimeter-sized, elongate and/or irregular coalesced type. Locally in small intervals (i.e., 2.56–2.61 mbsf), the vesicles are filled with bioclastic sediment (Figure **F2C**). From 3.42 to 3.70 mbsf, consolidated biodetrital grainstone was recovered that consists of various bioclasts, intraclasts, and volcaniclastics (Figure **F2D**). From 3.70 to 12.43 mbsf (base of the hole), the lava is porphyritic (up to 10% by volume of olivine and clinopyroxene) with an aphanitic groundmass (Figure **F2E**) and round, millimeter-sized pores. Coalesced vesicles are also observed (e.g., 6.56–6.66 mbsf). Within this lava interval, several shorter intervals of reddish stained volcanic breccia are observed (e.g., 8.10–8.20 mbsf; Figure **F2F**), some more strongly welded than others (e.g., 3.68–4.48 mbsf; Figure **F2G**).

3. Physical properties

Physical properties data for Site M0100 are shown in Table **T2** in the Site M0096 chapter (Webster et al., 2025b). Note that the thin overlying carbonate deposits were only measured for color reflectance; thus, the boundary between carbonates to lava is not covered by other physical properties data.

3.1. Hole M0100A

A total of 6.85 m of core from Hole M100A was scanned with the multisensor core logger (MSCL), and because the core exhibited moderate drilling-induced disturbance, 46% of the acquired data passed QA/QC (see Table **T10** in the Expedition 389 methods chapter [Webster et al., 2025a]). A total of six discrete samples were taken for *P*-wave and moisture and density (MAD) measurements. Digital linescans, color reflectance, and hyperspectral imaging were acquired on all cores.

3.1.1. Density and porosity

Data for density and porosity measurements are presented in Figures **F1** and **F3**. MSCL density measurements range 1.02–2.80 g/cm^3. Drilling-induced disturbance and short core lengths compromised data quality (see **Physical properties** in the Expedition 389 methods chapter [Webster et al., 2025a]) and limited sampling. A total of six discrete samples were analyzed for MAD, giving a bulk density range of 2.29–2.51 g/cm^3. Porosity values for the same samples range 14.1%–24.8%, and grain density values range 2.646–2.862 g/cm^3.

3.1.2. *P*-wave velocity

MSCL *P*-wave velocity measurements yielded no data. A total of six samples were measured using the discrete *P*-wave logger. Dry measurement values range 2078–4772 m/s (Figure **F4**). *P*-wave

velocity recorded for the samples after resaturation range 3051–5136 m/s. Because of the small number of *P*-wave data points available, no downhole trends are apparent.

3.1.3. Thermal conductivity

Thermal conductivity was measured on one core (see Table **T11** in the Expedition 389 methods chapter [Webster et al., 2025a]) with a value of 1.505 W/(m·K).

3.1.4. Magnetic susceptibility

MSCL magnetic susceptibility data range 20.39 × 10^{-5} to 540.81 × 10^{-5} SI (Figure **F1**). However, most of the magnetic susceptibility values fall between 100 × 10^{-5} and 300 × 10^{-5} SI with an average value for the hole of 165.14 × 10^{-5} SI. There are no apparent downhole trends.

3.1.5. Electrical resistivity

MSCL noncontact resistivity measurements yielded data ranging 1.42–124.53 Ωm, with most of the values in the range of 2–10 Ωm (Figure **F1**). There is no apparent downhole trend.

3.1.6. Natural gamma radiation

MSCL natural gamma radiation measurements display values ranging 27–35 counts/s and show no significant downhole trend (Figure **F1**).

3.1.7. Digital linescans, color reflectance, and hyperspectral imaging

All cores were digitally scanned, measured for color reflectance (where appropriate), and imaged with the hyperspectral scanner (see HYPERSPECTRAL in **Supplementary material**). Color

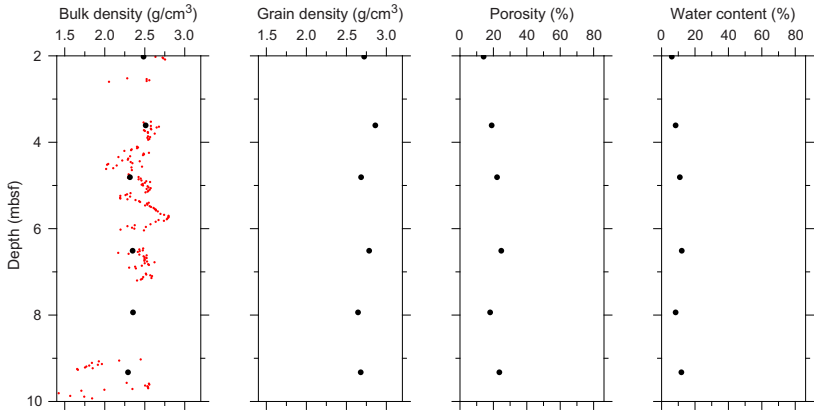

Figure F3. Physical properties, Hole M0100A. Black = discrete samples, red = MSCL.

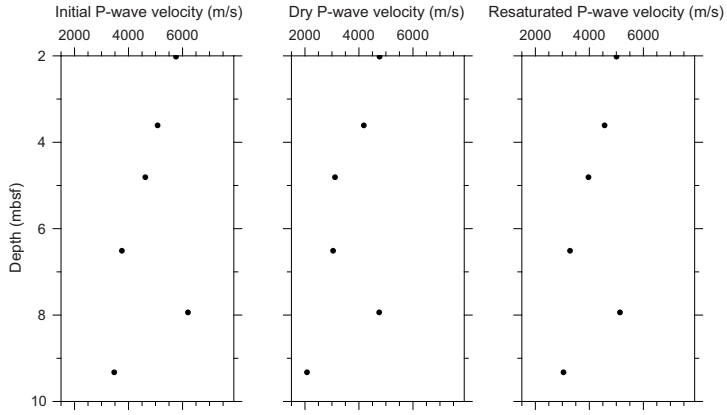

Figure F4. Initial, dry, and resaturated *P*-wave velocities measured on discrete samples, Hole M0100A.

reflectance L* values vary between 10.12% and 97.26% (Figure **F1**), a* varies between –1.26 and 4.17, b* varies between –0.81 and 18.09, and a*/b* varies between –1.15% and 3.88%. High to low values in color reflectance reflect a change in lithology from detrital to lava (Figure **F1**).

4. Geochemistry

4.1. Interstitial water

No interstitial water samples were collected from Site M0100.

4.2. Surface seawater

One surface seawater sample was collected from Site M0100 using a Niskin bottle deployed from the side of the vessel (see Figure **F22** in the Expedition 389 methods chapter [Webster et al., 2025a]). The salinity, pH, alkalinity, and ammonium concentration were analyzed off shore, and major cations and anions were measured during the Onshore Science Party. The salinity, pH, alkalinity, ammonium, and major element chemistry measured for this sample are consistent with the other surface seawater samples taken during Expedition 389 and align with the expected values for conservative elements in seawater (see Tables **T15** and **T17** in the Expedition 389 methods chapter [Webster et al., 2025a]); however, Site M0100 has the lowest measured surface water values for Ca, K, Mg, Na, S, and Sr of any samples measured during Expedition 389.

4.3. Bulk sediment and rocks

One basalt sample was analyzed for mineralogy and elemental composition (Sample 389-M0100A-9R-1, 21–24 cm; 10.18 mbsf) (see Figure **F10** in the Expedition 389 methods chapter [Webster et al., 2025a]). A second sample (389-M0100A-5R-2, 119–122 cm) is recorded in the Mobile Drilling Information System (mDIS) as submitted for mineralogy and elemental composition. However, no mineralogy or elemental abundance results are reported because the physical sample was not transferred to the laboratory.

4.4. Mineralogy

The basalt sample from Hole M0100A (389-M0100A-9R-1, 21–24 cm; 10.18 mbsf) is composed of plagioclase (61%) and pyroxene (39%) (Table **T2**). Presence of enstatite (orthopyroxene = 6%) is noted in the X-ray diffraction (XRD) results, plus a 1:1 forsterite-diopside olivine-clinopyroxene) ratio (see **Geochemistry** in the Expedition 389 methods chapter [Webster et al., 2025a]).

4.5. Elemental abundances

The elemental composition (Table **T3**) of the basalt sample (389-M0100A-9R-1, 21–24 cm; 10.18 mbsf) contains 54,718 mg/kg Ca, 53,846 mg/kg Mg, 1,379 mg/kg Mn, 543 mg/kg Sr, 72,232 mg/kg Al, and 82,628 mg/kg Fe. Other elements (Ba, Br, K, P, S, Ti, Zr, Cr, Cu, Ni, Rb, V, and Zn) are minor constituents or are below detection in the sample.

4.6. Carbon content

The results for total organic carbon (TOC), total carbon (TC), and total inorganic carbon (TIC) at Site M0100 are presented in Table **T4**. The basalt sample (389-M0100A-9R-1, 21–24 cm; 10.18 mbsf) contains 0.74% TC, 0.16% TOC, and 0.58% TIC.

Table T2. HighScore XRD mineral abundances, Site M0100. **Download table in CSV format.**

Table T3. Solid-phase elemental abundances, Site M0100. **Download table in CSV format.**

Table T4. TOC, TIC, and TC, Site M0100. **Download table in CSV format.**

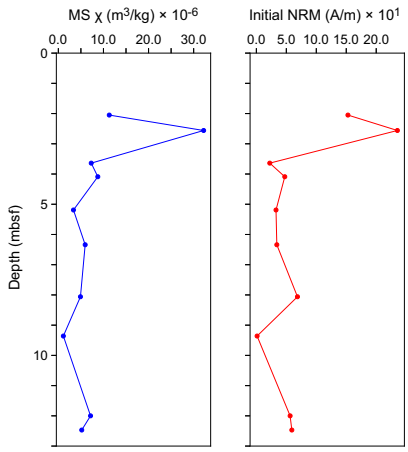

Figure F5. Magnetic susceptibility (MS) and NRM, Hole M0100A.

5. Paleomagnetism

A total of 10 plug samples were obtained from Hole M0100A. Measurements of low-field and mass-specific magnetic susceptibility (χ) were carried out for all samples. Initial natural remanent magnetization (NRM) was measured for all samples, as well as remanence following stepwise alternating field (AF) demagnetization up to a peak AF of 100 mT. For further details, see **Paleomagnetism** in the Expedition 389 methods chapter (Webster et al., 2025a).

5.1. Hole M0100A

A total of 10 lava samples were taken from Hole M0100A. High positive χ values occur throughout, ranging 1.11×10^{-6} to 32.2×10^{-6} m^3/kg with an arithmetic mean of 8.72×10^{-6} m^3/kg. The initial NRM intensity ranges 0.12–23.5 A/m with an arithmetic mean of 7.10 A/m. There is a peak located at 2.57 mbsf (Sample 3R-1, 7.5–10 cm) with high χ and NRM values (Figure **F5**). Patterns in χ and initial NRM are relatively synchronous, suggesting that magnetic concentration and properties drive these variations.

6. Geochronology

One U-Th date was obtained from a Hole M0100A sample (1R-1, 4–5 cm); it was not rejected (see Table **T21** in the Expedition 389 methods chapter [Webster et al., 2025a]) and yielded a date of ~329 ky BP (see Table **T22** in the Expedition 389 methods chapter [Webster et al., 2025a]). This date is consistent with the estimated Marine Isotope Stage 9 age for the H6 terrace (Ludwig et al., 1991; Webster et al., 2009 and references therein).

References

Ludwig, K.R., Szabo, B.J., Moore, J.G., and Simmons, K.R., 1991. Crustal subsidence rate off Hawaii determined from $^{234}U/^{238}U$ ages of drowned coral reefs. Geology, 19(2):171–174. **https://doi.org/10.1130/0091-7613(1991)019<0171:CSROHD>2.3.CO;2**

Webster, J.M., Braga, J.C., Clague, D.A., Gallup, C., Hein, J.R., Potts, D.C., Renema, W., Riding, R., Riker-Coleman, K., Silver, E., and Wallace, L.M., 2009. Coral reef evolution on rapidly subsiding margins. Global and Planetary Change, 66(1–2):129–148. **https://doi.org/10.1016/j.gloplacha.2008.07.010**

Webster, J.M., Ravelo, A.C., Grant, H.L.J., and the Expedition 389 Scientists, 2025. Supplementary material, **https://doi.org/10.14379/iodp.proc.389supp.2025**. In Webster, J.M., Ravelo, A.C., Grant, H.L.J., and the Expedition 389 Scientists, Hawaiian Drowned Reefs. Proceedings of the International Ocean Discovery Program, 389: College Station, TX (International Ocean Discovery Program).

Webster, J.M., Ravelo, A.C., Grant, H.L.J., Rydzy, M., Stewart, M., Allison, N., Asami, R., Boston, B., Braga, J.C., Brenner, L., Chen, X., Chutcharavan, P., Dutton, A., Felis, T., Fukuyo, N., Gischler, E., Greve, S., Hagen, A., Hamon, Y., Hathorne, E., Humblet, M., Jorry, S., Khanna, P., Le Ber, E., McGregor, H., Mortlock, R., Nohl, T., Potts, D., Pro-

haska, A., Prouty, N., Renema, W., Rubin, K.H., Westphal, H., and Yokoyama, Y., 2025a. Expedition 389 methods. In Webster, J.M., Ravelo, A.C., Grant, H.L.J., and the Expedition 389 Scientists, Hawaiian Drowned Reefs. Proceedings of the International Ocean Discovery Program, 389: College Station, TX (International Ocean Discovery Program). **https://doi.org/10.14379/iodp.proc.389.102.2025**

Webster, J.M., Ravelo, A.C., Grant, H.L.J., Rydzy, M., Stewart, M., Allison, N., Asami, R., Boston, B., Braga, J.C., Brenner, L., Chen, X., Chutcharavan, P., Dutton, A., Felis, T., Fukuyo, N., Gischler, E., Greve, S., Hagen, A., Hamon, Y., Hathorne, E., Humblet, M., Jorry, S., Khanna, P., Le Ber, E., McGregor, H., Mortlock, R., Nohl, T., Potts, D., Prohaska, A., Prouty, N., Renema, W., Rubin, K.H., Westphal, H., and Yokoyama, Y., 2025b. Site M0096. In Webster, J.M., Ravelo, A.C., Grant, H.L.J., and the Expedition 389 Scientists, Hawaiian Drowned Reefs. Proceedings of the International Ocean Discovery Program, 389: College Station, TX (International Ocean Discovery Program). **https://doi.org/10.14379/iodp.proc.389.103.2025**